Intelligent Wheelsets for the trains of the future: the role of in-service wheel-rail force measurement

Flavio Velletrani[1], Riccardo Licciardello[1], Massimiliano Bruner[1]
[1]*DICEA Civil, Building and Environmental Engineering Dpt., SAPIENZA University of Roma (Italy)*
DICEA Dipartimento di Ingegneria Civile, Edile e Ambientale, SAPIENZA University of Roma (Italia)

SUMMARY

The European rail sector has a strong interest in innovations for monitoring the operational condition of a running vehicle. Many high technology systems can lead up to future rail systems relying on “intelligent vehicles”. This document describes the conceptual development of a monitoring system based on FEM calculations. The system uses signals from wheel-fitted transducers. The signals are processed with the main aim of increasing design and maintenance effectiveness through a better knowledge of in-service loads, supporting predictive maintenance through the early identification of faults, and identifying safety hazards.

INTRODUCTION

The European rail sector has always paid attention to innovations regarding “health monitoring” of trains' running gear, that could lead up to future rail systems relying on highly “intelligent vehicles”. Health monitoring systems, based on the analysis of operational data carried by signals from transducers applied on the running gear, have the main aims of:

a) increasing design and maintenance effectiveness;

b) supporting predictive maintenance through the early identification of faults;

c) identifying safety hazards.

In this context, the RUN2Rail project (2017-2019), funded by SHIFT2RAIL, has produced several technology concepts, including the one developed by the authors. The starting idea was to simplify the Corazza-Malavasi-Licciardello Methodology – (below referred to as CML method) developed over the years by SAPIENZA University of Rome. The CML method was originally intended for highly accurate measurements of wheel-rail forces - for example for research and vehicle acceptance purposes. For in-service monitoring the requirement of a low number of telemetry channels takes priority over accuracy. Therefore, several different simplified gauge configurations were explored by analysing the results of a validated Finite Element Model of a high-speed-train wheel in order to quantify their accuracy and select the best one. The hardware assumed for the system is already being tested in service by another partner of RUN2Rail. The main idea in the project was to explore the suitability of the system for increased design effectiveness - item a) above. In this paper the role of the system is examined more in detail also for items b) and c).

1. STATE OF THE ART

The European rail sector has a strong interest in innovations for condition monitoring - or “health monitoring” - systems of the trains' running gear, leading up to future rail systems relying on highly

intelligent vehicles. This is testified by SHIFT2RAIL's Multi-Annual Action Plan [1] which foresees the integration of advanced sensor-based health monitoring systems in the running gear with the next generation of Train Control and Monitoring Systems (TCMS). Such monitoring systems rely on sensors or transducers on the running gear itself, whose signals may in principle be processed with the following aims:

a) increasing design and maintenance effectiveness;

b) supporting predictive maintenance through the early identification of faults;

c) identifying safety hazards.

The knowledge of in-service loads is a valuable contribution to the design and maintenance of railway vehicle components (item a), particularly wheelsets, bogie frames and other running-gear components but also of the car-body. Generally, the design loads are standardised. The wheelset design process in the European standards are focused on the actions given by press-fitting the wheel and brake discs on the axles (EN 13260 [2]), as well as on the fatigue given by alternate bending when running (EN 13103-1 [3]). For the latter aspect, wheel longitudinal, lateral and vertical loads are important. The design wheel-rail contact loads are chosen as a multiple of nominal loads, and the design process considers them as constant values. Standardised load values have to be conservative as they must represent a large variety of possible cases (lines with many or few curves, types of track and track components, frequent or rare traction/braking, etc.).

With the current state-of-the-art, wheel load measurement systems are however quite complex and not well suited to unattended, durable and widespread measurement on a fleet of trains. The measurements are usually performed by means of strain gauges applied to the wheel and/or the axle. Several methods have been developed through the years, all with the requirement of quite high sensitivity and accuracy, since they are routinely used when placing a vehicle type on the market with the purpose of assessing running safety and track loading (in the European legislation: standard EN 14363 [4]). A telemetry is required to transmit the signals from the rotating wheel/wheelset to the on-board part of the measurement chain. Accurate reviews of the state of the art have been given firstly by Otter et al. [5] and, more recently, by Bracciali et al. [6] looking into the main requirements and referenced to technical regulations.

A promising alternative to strain-gauge methods that lends itself to routine in-service measurement is the measurement of lateral loads through the lateral deflection of the wheel by means of proximity sensors as described by Matsumoto et al. [8]. In this application the longitudinal and vertical components are measured through suspension deflection. The intended purpose is safety-related (item c. above). The loads are measured in order to monitor the derailment ratio (lateral wheel load divided by vertical load) on 2 wheelsets of one of the trainsets in service.

Regarding purpose b), systems exist or are being studied to identify a variety of running-gear faults.

Instability caused by high equivalent conicity/high speeds is usually detected by on-bogie frame accelerometers [8] and translated into operational measures (slowing down the train). Suspension faults may change stiffness/damping values; i.e. dampers' efficiency may significantly change the running dynamics [9], and wheel load unbalances potentially affecting running safety may occur. Wheel defects such as flats and out-of-roundness impart high dynamic loads on the infrastructure [10].

On-board accelerometers may provide useful information for their identification. Gearbox faults may cause operational unavailability due to the train being withdrawn from service and, if severe, also safety issues. Gearbox monitoring is currently performed with different systems based on e.g.

temperature measurement [11]. Axle-box temperatures are also measured for monitoring purposes ([12], [13]).

2. DEVELOPMENT OF THE IN-SERVICE FORCE MONITORING CONCEPT

2.1 Objectives of the research work

In the work described here, the main objective is the assessment of the feasibility of simple low-cost wheel-load strain-gauge-based measurement systems with the potential for routine in-service application. The concept is dubbed Wheel/wheelset In-Service Force Monitoring (WISE-FM).

A high-accuracy system developed at SAPIENZA University of Rome for research and vehicle acceptance purposes, the CML method ([14], [15]) was a starting point. It is a wheel-based strain-gauge method providing Distance-Based Sampling – i.e. with a fixed number of samples per metre, rather than per second – of force components. For vehicle acceptance purposes it requires 12 telemetry channels per wheel. Using, and extending, the principles upon which the CML method was developed, the idea was to screen several strain-gauge configurations to understand if there are configurations that provide a sufficient accuracy for WISE-FM with a much lower number of channels per wheel (ideally only one).

Section 2.2 describes the Finite Element Model and the screening process used to identify strain-gauge configurations with acceptable accuracy. Section 2.3 quantifies the accuracy achievable with the selected configuration. It shows, through dynamic considerations, to what extent impact loads should be detectable. In section 3 the suitability of a WISE-FM system with the determined accuracy in fulfilling the above purposes is discussed. Section 5 provides conclusions and recommendations for further research.

2.2 FEM Procedure

The accuracy achievable with different strain gauge configurations is investigated through several structural simulations, in order to identify suitable bridge configurations and gauge positions.

The case study is a previously validated linear FEM code model [19], applied to a Lucchini – Alstom wheel, belonging to a wheelset of the ETR460 class Pendolino trainset (Fig. 1), at the same time analysed experimentally on a test rig [15]. The model is based on the use of octahedral brick elements, covered with shell elements connected to the volume mesh nodes, to simulate the strain gauge behaviour. Radial strains were further exported through 8 (quasi) radial paths applied every 45° at both surfaces (inner – outer) of the wheel disc and analysed in order to find suitable measurement points, below named A-B-C-D. An estimation of strain gauge signal behaviour along the wheel revolution is obtained by means of circular paths.

The complete model linearity reduced the amount of simulations, so several load cases were obtained through linear combination of simulated ones.

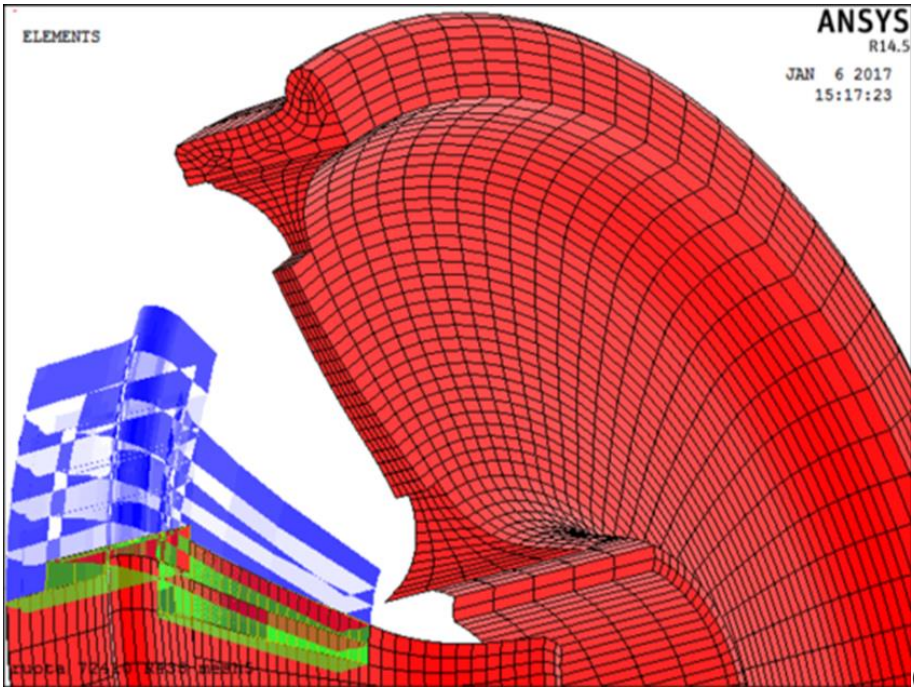

(a)

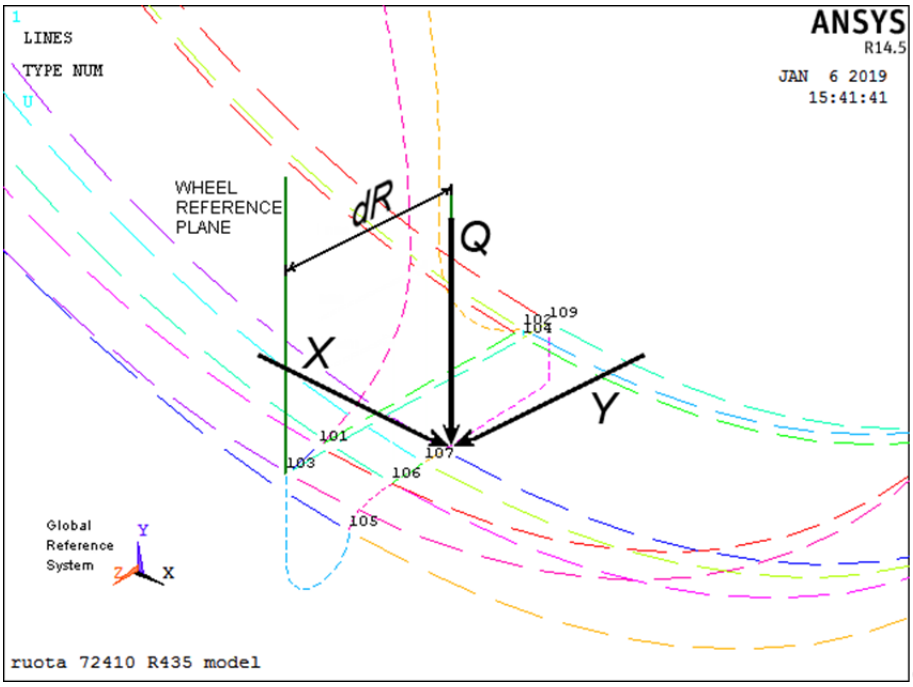

(b)

Figure 1 – FE model of Lucchini – Alstom wheel 72410: (a) wheel section view, use of octahedral brick elements in code FEM structure; (b) wheel-rail contact forces (in this case applied on wheel rim) positioned at distance dR from the wheel's reference plane: X longitudinal force, Q vertical wheel load, Y lateral force

Input for load combinations and load distributions has been taken from the Widem Project [16], which investigated the running dynamic behaviour of a Pendolino trainset having very similar wheelsets. The contact point for the wheel load (X, longitudinal; Q vertical; Y lateral forces) is identified by the dR parameter, that describes its distance from the wheel reference plane. For this case study, three contact points have been considered on the wheel, related to three usual wheel-rail contact conditions: the first on the flange, the second on the tread centre and the last on the outer zone of the tread. In order to follow the experimental laboratory tests, values for the three components Q and Y (Tab. 1) were chosen to obtain a linear increase for the vertical load, while Y

values modify their linearity due the combined effects of Q. On the other hand, the values of X were chosen to match available experimental results.

Load lateral position	dR	[mm]	**54**, **70**, **81**
Wheel load	Q	[kN]	50, **60**, 70, **80**, 90
Lateral contact force	Y	[kN]	**0**, 3, 7, 14, 30, 50, **80**
Longitudinal contact force	X	[kN]	**0**, **16**, **32**, 35, 50

Table 1 – Review of FEM conditions tests: force values and application points; in bold the simulations performed; the other ones are used to extend and validate model linearity

Simulation results allowed the optimal position for the strain gauge transducers to be fixed on the wheel web: a web circle-radius can be identified to define maximum radial deformation. Suitable wiring configurations, between strain gauges, have been conceptualised and a corresponding calibration constant K obtained that fits the variability of wheel-rail contact patch position for each vehicle running condition. In order to avoid complex post-processing algorithms, a generic force component is required to be calculated in real-time from the measured strains as:

$$F = \frac{1}{K_{B,P}} \cdot \varepsilon_{R,P}$$

where B represents the generic bridge configuration, applied on the generic radius R. Consequently, $\varepsilon_{R,P}$ is the equivalent (quasi-) radial strain given by the Wheatstone bridge with gauges applied in the generic set of points P. For a typical 4-strain-gauge (SGi i=1..4) bridge (Fig. 2) the equivalent strain is:

$$\varepsilon_{R,P} = \varepsilon_{SG1} - \varepsilon_{SG2} + \varepsilon_{SG3} - \varepsilon_{SG4}$$

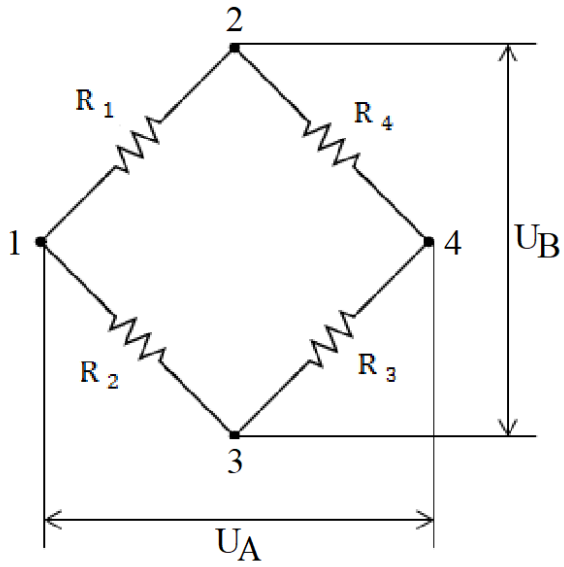

Figure 2 – Wheatstone classical bridge scheme: R1…R4 strain gauges connected in 1...4 nodal points, UB bridge input voltage, UA bridge output voltage (measurement signals ε_{SG1}, ε_{SG2}, ε_{SG3}, ε_{SG4})

The Wheatstone bridge simply “sums with sign” the strains in the points where the gauges are applied.

The temperature effects are assumed to be compensated by the bridge configurations. This assumption is reasonable for bridges whose gauges are applied all to one side of the wheel (particularly the inner side which is always well shaded from sunlight).

For the sought component of wheel-rail contact force component *F,* the calibration constant $K_{B,P}$, where B is the specific (full or half) bridge configuration applied in points P on the wheel web located at radius R, is calculated through the following formula:

$$K_{B,P} = \frac{1}{F}\bar{\varepsilon}_R = \frac{1}{F}\frac{1}{n}\sum_j \varepsilon_{R,P,j}\left(F, \underline{G}, dR_j\right)$$

$K_{B,P}$ is a function of:

- *F*, component of contact force to be measured (e.g. *Q)*;
- $\underline{G}$, vector of influence forces (the other 2 components), e.g. (*Y*, *X*) when F (e.g. *Q)* is measured;
- dR_j wheel-rail contact point distance from wheel reference plane (at the gauge-side of the flange).

Therefore, the parasitic effects induced on the measurement of the single contact force components (Q, Y, X) are considered in the evaluation of the calibration coefficient $K_{B,P}$, without managing the variability of each individual signal (i.e. that given by the sample dispersion of the values ε_{SG1}, ε_{SG2}, ε_{SG3}, ε_{SG4}). The corresponding measurement uncertainty is derived using the simulation results, based on the variability of the general relationship: this derivation (i.e. the determination of the calibration constant) represents the core of the procedure.

The procedure yields a calibration constant that minimises errors for a specific contact-point position (in this work for dR_j=70 mm). Future experimental results could suggest a better choice of the contact point depending on the application.

The simulations provide the value $F_{meas,j}$ that would be measured by a system on a running wheel, in which the above calibration constant is used according to the actual load conditions:

$$F_{meas,j} = \frac{1}{K_{B,P}}\varepsilon_{R,P,j}\left(F, \underline{G}, dR_j\right)$$

The difference $F_{meas,j} - F$ is an estimate for the error of the measurement system in the specific loading conditions. The following two criteria are considered as necessary and sufficient for the measurement to be assessed as sufficiently accurate:

$$E = \left|\frac{1}{n}\sum_j \left(F_{meas,j} - F\right)\right| < E_{max}$$

and

$$\sigma = \sqrt{\frac{\left(F_{meas,j} - F\right)^2}{n-1}} < \sigma_{max}$$

Both E_{max}, σ_{max} limit values are set to 10% according to experimental results ([14], [15], [16], [17]). The results of the above calculations are summarised in table form (Tab. 2) below, for the different SG configurations (Tab. 3).

DIAMETRAL FULL BRIDGE_vertical section, Wheel inner side
Model calibration values Q=70 [kN]; Y=0 [kN] , 50 [kN], X=50 [kN]
Strain gauge radial position = 174 [mm]

Point A, radial position = 174 [mm] Load conditions					Detected	Q "meas" =	ε /Kb (Q) -	(ε /Kb (Q) -	Y "meas" =	ε /Kb (Y) -	(ε /Kb (Y) -	X "meas" =	ε /Kb (X) -	(ε /Kb (X) -
Test #	Q [kN]	Y [kN]	X [kN]	dR [mm]	strain [με]	ε /Kb (Q)	Q	Q)^2	ε /Kb (Y)	Y	Y)^2	ε /Kb (X)	X	X)^2
1	70	0	50	70	**85**	79	9	90	-2	-2	6	N/A	N/A	N/A
2	70	50	50	70	**-1676**	-1569	-1639	2685995	48	-2	6	N/A	N/A	N/A
3	70	0	50	54	**-1**	-1	-71	5044	0	0	0	N/A	N/A	N/A
4	70	50	50	54	**-1767**	-1654	-1724	2972288	50	0	0	N/A	N/A	N/A
5	70	0	50	81	**141**	132	62	3788	-4	-4	16	N/A	N/A	N/A
6	70	50	50	81	**-1620**	-1516	-1586	2514889	46	-4	16	N/A	N/A	N/A
Avg Error[με] and **Std. Dev [με]** on all 6 test							-825	**1279**		-2	**3**			N/A

NB: the parameters' calculation related to contact force X is not applicable (N/A), since the radial strain effects are nil at the measuring points on the vertical radii of the wheel disk.

Point B, radial position = 307 [mm] Load conditions					Detected	Q "meas" =	ε /Kb (Q) -	(ε /Kb (Q) -	Y "meas" =	ε /Kb (Y) -	(ε /Kb (Y) -	X "meas" =	ε /Kb (X) -	(ε /Kb (X) -
Test #	Q [kN]	Y [kN]	X [kN]	dR [mm]	strain [με]	ε /Kb (Q)	Q	Q)^2	ε /Kb (Y)	Y	Y)^2	ε /Kb (X)	X	X)^2
1	70	0	50	70	**-261**	69	-1	1	-102588	-102588	10524365873	N/A	N/A	N/A
2	70	50	50	70	**-261**	69	-1	1	-102536	-102586	10523889052	N/A	N/A	N/A
3	70	0	50	54	**-288**	76	6	39	-112927	-112927	12752586542	N/A	N/A	N/A
4	70	50	50	54	**-287**	76	6	38	-112878	-112928	12752746270	N/A	N/A	N/A
5	70	0	50	81	**-243**	65	-5	30	-95548	-95548	9129405918	N/A	N/A	N/A
6	70	50	50	81	**-243**	64	-6	31	-95500	-95550	9129714878	N/A	N/A	N/A
Avg Error[με] and **Std. Dev [με]** on all 6 test							0	**5**		-103688	**113853**			N/A

Point C, radial position = 351 [mm] Load conditions					Detected	Q "meas" =	ε /Kb (Q) -	(ε /Kb (Q) -	Y "meas" =	ε /Kb (Y) -	(ε /Kb (Y) -	X "meas" =	ε /Kb (X) -	(ε /Kb (X) -
Test #	Q [kN]	Y [kN]	X [kN]	dR [mm]	strain [με]	ε /Kb (Q)	Q	Q)^2	ε /Kb (Y)	Y	Y)^2	ε /Kb (X)	X	X)^2
1	70	0	50	70	**-244**	70	0	0	-12	-12	156	N/A	N/A	N/A
2	70	50	50	70	**730**	-210	-280	78282	37	-13	158	N/A	N/A	N/A
3	70	0	50	54	**-254**	73	3	9	-13	-13	169	N/A	N/A	N/A
4	70	50	50	54	**725**	-208	-278	77447	37	-13	164	N/A	N/A	N/A
5	70	0	50	81	**-233**	67	-3	9	-12	-12	143	N/A	N/A	N/A
6	70	50	50	81	**739**	-212	-282	79682	38	-12	147	N/A	N/A	N/A
Avg Error[με] and **Std. Dev [με]** on all 6 test							-140	**217**		-12	**14**			N/A

Point D, radial position = 210 +-10 [mm] Load conditions					Detected	Q "meas" =	ε /Kb (Q) -	(ε /Kb (Q) -	Y "meas" =	ε /Kb (Y) -	(ε /Kb (Y) -	X "meas" =	ε /Kb (X) -	(ε /Kb (X) -
Test #	Q [kN]	Y [kN]	X [kN]	dR [mm]	strain [με]	ε /Kb (Q)	Q	Q)^2	ε /Kb (Y)	Y	Y)^2	ε /Kb (X)	X	X)^2
1	70	0	50	70	**1**	5	-65	4249	0	0	0	N/A	N/A	N/A
2	70	50	50	70	**-1435**	-10996	-11066	122466124	48	-2	6	N/A	N/A	N/A
3	70	0	50	54	**-10**	-76	-146	21176	0	0	0	N/A	N/A	N/A
4	70	50	50	54	**-1703**	-13054	-13124	172236059	56	6	42	N/A	N/A	N/A
5	70	0	50	81	**37**	281	211	44396	-1	-1	1	N/A	N/A	N/A
6	70	50	50	81	**-1360**	-10422	-10492	110086054	45	-5	24	N/A	N/A	N/A
Avg Error[με] and **Std. Dev [με]** on all 6 test							-5780	**8998**		0	**4**			N/A

Results summary

Load conditions for all tests						Q int_Q70Y00dR70_x50			Y int_Q70Y00dR70_x50			X int_Q70Y00dR70_x50		
							Avg. Error			Avg. Error			Avg. Error	
Test #	Point	Q [kN]	Y [kN]	X [kN]	dR [mm]	Kt (Q)	Q [με]	Std Dev Q [με]	Kt (Y)	Y [με]	Std Dev Y [με]	Kt (Y)	Y [με]	Std Dev Y [με]
1; 2; 3; 4; 5; 6	**A**	70	0; 50	50	54;70;81	1.07	-825	**1279**	-35.25	-2	**3**	N/A	0	0
1; 2; 3; 4; 5; 6	**B**	70	0; 50	50	54;70;81	-3.77	0	**5**	0.00	-103688	**113853**	N/A	0	0
1; 2; 3; 4; 5; 6	**C**	70	0; 50	50	54;70;81	-3.48	-140	**217**	19.50	-12	**14**	N/A	0	0
1; 2; 3; 4; 5; 6	**D**	70	0; 50	50	54;70;81	0.13	-5780	**8998**	-30.17	0	**4**	N/A	0	0

Table 2 – Calculation summary table for Q = 70 kN, Avg Error and Std Dev highlighted in colour for each configuration

Table 3 – SG Bridge configuration summary

1. Single Strain Gauge - POINTS A-B-C-D_lower vertical section

Inner wheel side

Point	Kt (Q)	Q "meas"	Err%	Dev Std %	Kt (Y)	Y "meas"	Err%	Dev Std %	Kt (X)	X "meas"	Err%	Dev Std %
A	0.2744	70	1630%	2527%	-12.5237	50	3%	5%	0.0000	N/A	N/A	N/A
B	-1.7712	70	0%	11%	0.0000	50	N/A	N/A	0.0000	N/A	N/A	N/A
C	-1.5144	70	142%	221%	6.0314	50	35%	39%	0.0000	N/A	N/A	N/A
D	0.0087	70	N/A	N/A	-11.3465	50	0%	5%	0.0000	N/A	N/A	N/A

Admittable solution		
Q int	Y int	X int
-	TRUE	N/A
-	-	N/A
-	-	N/A
-	TRUE	N/A

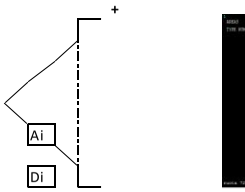

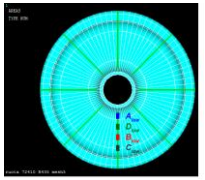

Acceptance Values Summary

Error %	min	max
|E %| < Vs%	0%	10%
Vs% < |E %| < Vamm%	10%	25%
Std. Dev. %		
|D std %| < Vs%	0%	10%
Vs% < |D std %| < Vamm%	10%	25%

2. DIAMETRAL FULL BRIDGE_vertical section

Inner wheel side

Point	Kt (Q)	Q "meas"	Err%	Dev Std %	Kt (Y)	Y "meas"	Err%	Dev Std %	Kt (X)	X "meas"	Err%	Dev Std %
A	1.0685	70	1178%	1827%	-35.2531	50	4%	6%	0.0000	N/A	N/A	N/A
B	-3.7712	70	0%	8%	0.0025	50	N/A	N/A	0.0000	N/A	N/A	N/A
C	-3.4807	70	200%	310%	19.5004	50	25%	27%	0.0000	N/A	N/A	N/A
D	0.1305	70	8258%	12855%	-30.1732	50	1%	8%	0.0000	N/A	N/A	N/A

Admittable solution		
Q int	Y int	X int
-	TRUE	N/A
TRUE	-	N/A
-	-	N/A
-	TRUE	N/A

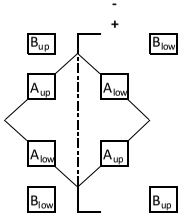

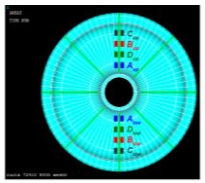

3. DIAMETRAL FULL BRIDGE_horizontal section

Inner wheel side

Point	Kt (Q)	Q "meas"	Err%	Dev Std %	Kt (Y)	Y "meas"	Err%	Dev Std %	Kt (X)	X "meas"	Err%	Dev Std %
A	0.0000	N/A	N/A	N/A	0.0000	N/A	N/A	N/A	0.9663	50	0%	76%
B	0.0000	N/A	N/A	N/A	0.0000	N/A	N/A	N/A	-1.4280	50	0%	5%
C	0.0000	N/A	N/A	N/A	0.0000	N/A	N/A	N/A	-1.3481	50	10%	45%
D	0.0000	N/A	N/A	N/A	0.0000	N/A	N/A	N/A	0.3914	50	0%	100%

Admittable solution		
Q int	Y int	X int
N/A	N/A	-
N/A	N/A	TRUE
N/A	N/A	-
N/A	N/A	-

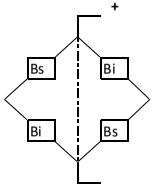

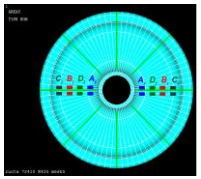

4. "L" FULL BRIDGE_lower vertical - right horizontal radii

Inner wheel side

Point	Kt (Q)	Q "meas"	Err%	Dev Std %	Kt (Y)	Y "meas"	Err%	Dev Std %	Kt (X)	X "meas"	Err%	Dev Std %
A	0.3295	70	2416%	3748%	-22.2915	50	2%	5%	-0.8561	50	728%	1259%
B	-3.6888	70	0%	14%	-0.0036	50	########	########	-0.7987	50	495%	552%
C	-2.9298	70	88%	137%	7.1948	50	57%	63%	-0.7618	50	167%	337%
D	-0.1332	70	5526%	8578%	-20.6166	50	1%	5%	0.3177	50	2202%	3431%

Admittable solution		
Q int	Y int	X int
-	TRUE	-
-	-	-
-	-	-
-	TRUE	-

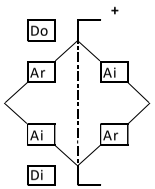

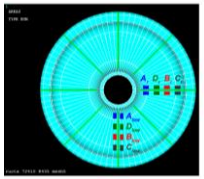

5. CROSS FULL BRIDGE

Inner wheel side

Point	Kt (Q)	Q "meas"	Err%	Dev Std %	Kt (Y)	Y "meas"	Err%	Dev Std %	Kt (X)	X "meas"	Err%	Dev Std %
A	-1.7325	70	96%	150%	-4.6650	50	52%	58%	0.0000	50	78689%	118845%
B	-0.4817	70	2%	218%	-0.0243	50	2775%	6776%	0.0143	50	18511%	22129%
C	-1.1895	70	51%	84%	0.0638	50	1336%	2161%	0.0000	N/A	N/A	N/A
D	-0.2830	70	576%	896%	-4.5679	50	9%	11%	-0.0012	50	144021%	210193%

Admittable solution		
Q int	Y int	X int
-	-	-
-	-	-
-	-	-
-	-	-

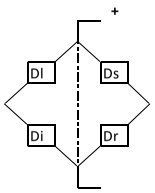

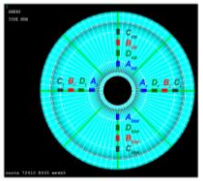

6. Combination of A and C (to maximize Y and neglet Q)

A+C (FB opposite sides), A-C (HB -adjacent sides); Ai-Ci+As-Cs; Ai+Ci-As-Cs

Inner wheel side

Config	Kt (Q)	Q "meas"	Err%	Dev Std %	Kt (Y)	Y "meas"	Err%	Dev Std %	Kt (X)	X "meas"	Err%	Dev Std %
A-C	1.7888	70	370%	574%	-18.5551	50	13%	15%	0.0000	N/A	N/A	N/A
A+C	-1.2400	70	187%	292%	-6.4924	50	27%	31%	0.0000	N/A	N/A	N/A
Ai-Ci+As-Cs	3.5776	70	370%	574%	-37.1103	50	13%	15%	0.0000	N/A	N/A	N/A
Ai+Ci-As-Cs	-2.4799	70	187%	292%	-12.9847	50	27%	31%	0.0000	N/A	N/A	N/A

Admittable solution		
Q int	Y int	X int
-	-	-
-	-	-
-	-	-
-	-	-

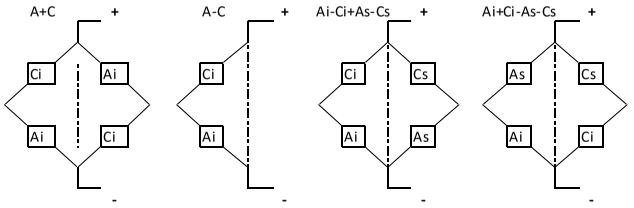

The choice of the points in which the strain gauges are applied are based on key points of the radial strain patterns, as highlighted in Fig. 3 for the "candidate" measurement points. For example, $\varepsilon_{R,A}$ represents the radial (R) strain evaluated at point A.

a) A: $\varepsilon_{R,A} = \varepsilon_{R,max}$ maximum strain, and maximum sensitivity to *Y*. A small effect of *Q*, (related to *dR*) is in any case detected.

b) B: $\varepsilon_{R,B} = \varepsilon_R(Q, dR)$ strain independence from *Y*, only Q is detected with no practical influence of *dR* on its radial position;

c) C: $\varepsilon_{R,C} = \varepsilon_{min}$ local minimum of *Y* strain pattern (strain of opposite sign respect to the one in A), in the area between *B*-circle and rim;

d) D: $\varepsilon_{R,D} = \varepsilon_R(Y, dR)$ strain independence from *Q*; since its radial position is strongly influenced by *dR*, a reference position for *D* is needed, so the radius corresponding to the centered axle condition (dR=70) was chosen.

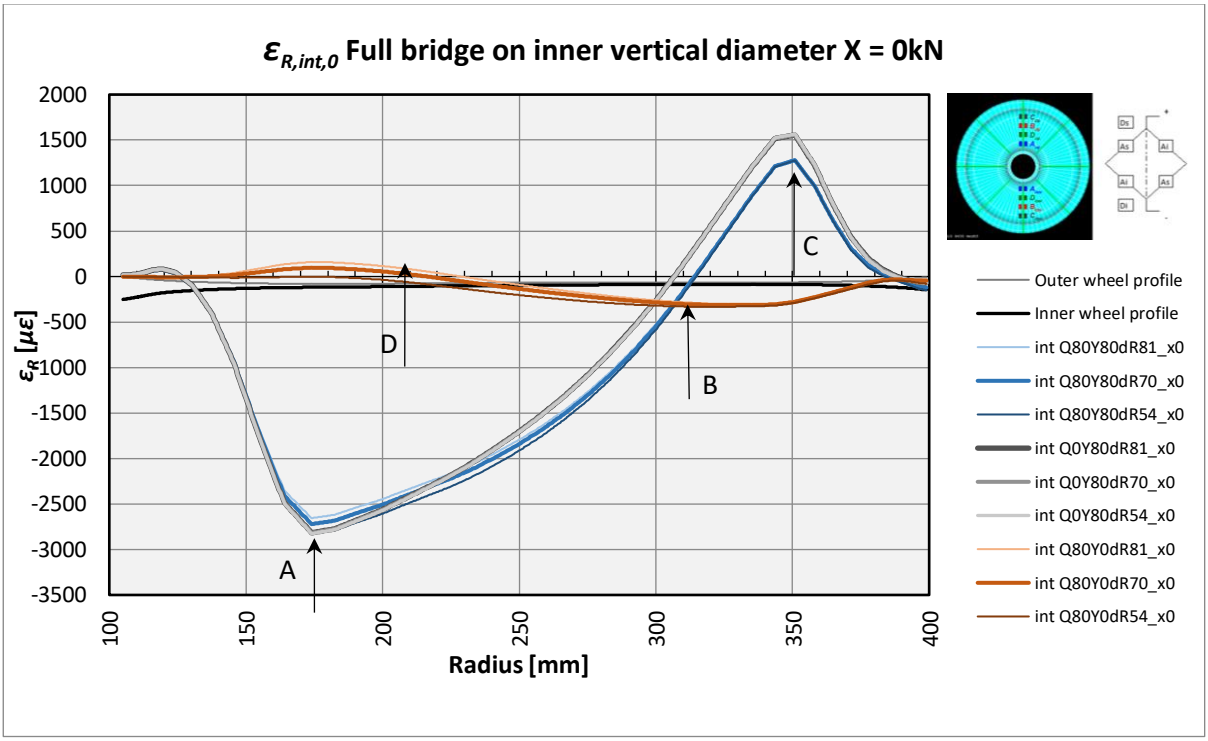

Figure 3 – Equivalent radial strain $\varepsilon_{R,int,0}$ for a full bridge simulation (inner side of wheel disc - int):Q=80 kN; Y=0 kN,80 kN; X = 0kN; dR=54 mm, 70 mm, 81 mm, radial position of strain gauges x0: 0°, 180°. The strain gauge radial positions were identified with the help of indications derived from points A, B, C, D as described above.

2.3 Achievable accuracy for the different strain gauge configurations

2.3.1 Results of the static modelling

The screening described above led to the conclusion that no 1-channel/wheel configuration satisfied the acceptance criteria for Distance Based Sampling (DBS) (n. 1 on Tab. 3). The main uncertainty causes for these configurations were the coupling of Q, Y and the asymmetry of the strain field due to X. None of the combinations shown above led to the identification of a constant calibration factor (K_B) characterised by acceptable error.

Bridges with gauges at different radii alternately measuring different force components were also explored (n. 6 of Tab. 3); no relevant results were achieved because of the coupling of the force components and the influence of dR.

As a following step, 2-channel/wheel configurations were explored (n. 2 – 3 – 4 – 5 of Tab. 3), with more significant results. Different configurations achieved the requirements, resulting suitable mainly for the inner side of the wheel, specifically the requirements for Y were achieved by two schemes (n. 2 – 3), whereas only one scheme (n. 2) was appropriate for measuring Q. So, the simplest configuration (n. 2) proves to be the most suitable and flexible: diametric full bridge, connecting strain gauges on opposite radii on adjacent sides of the bridge, all on the inner side of the wheel (see Fig. 4). The same configuration on the outer wheel side was less successful. A subset of the calculated errors for the bridges in the vertical and horizontal positions are shown (Tab. 4). M To sum up, the measurement of Q and Y with good accuracy is possible when the instrumented diameter is vertical.

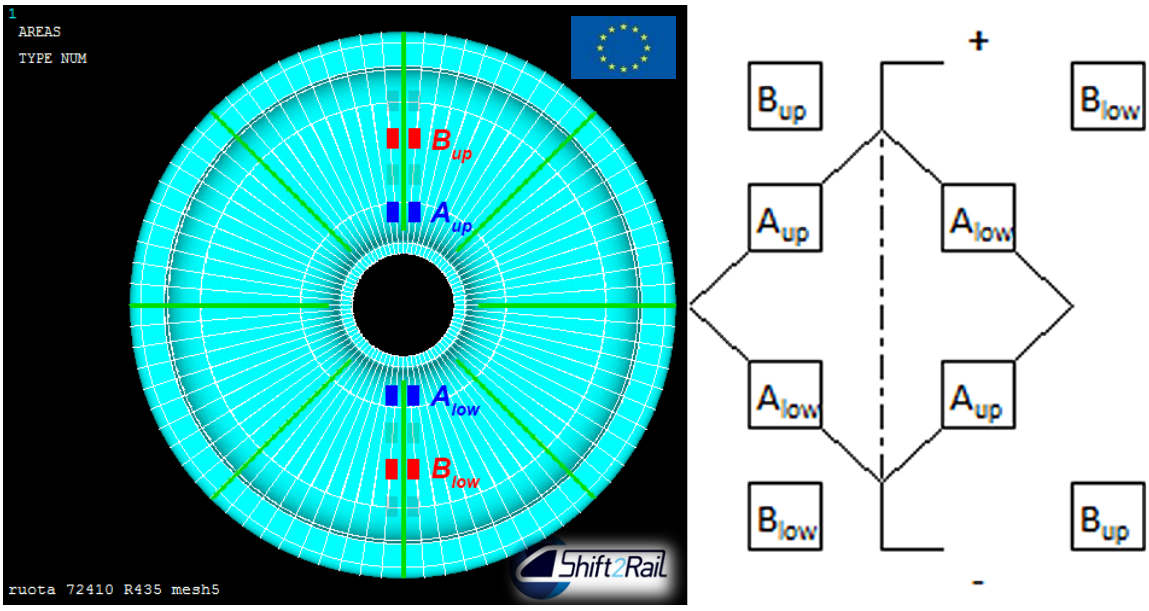

Figure 4 – Adopted configuration: Full Bridges respectively in A (Y) and B (Q, X) on the inner side of the wheel

	Selected scheme: Full bridge (P_{low} – P_{up}) on the inner side of the wheel											
	Q: FB on vertical plane				Y: FB on vertical plane				X: FB on horizontal plane			
Point	Kt (Q)	Q mis	Err %	Dev Std %	Kt (Y)	Y mis	Err %	Std dev %	Kt (X)	X mis	Err %	Std dev %
A	1.069	70	1178%	1827%	-35.253	50	4%	6%	0.966	50	0%	76%
B	-3.771	70	0%	8%	0.003	50	>10^5	>10^5	-1.428	50	0%	5%
C	-3.481	70	200%	310%	19.500	50	25%	27%	-1.348	50	10%	45%
D	0.131	70	8258%	12855%	-30.173	50	1%	8%	0.391	50	0%	100%

Table 4 – Configuration screening for Q = 70kN, Q, Y sampled on the vertical plane, X sampled on the horizontal one (config. 2, 3 of Fig. 2)

It was also discovered during the RUN2Rail work that this configuration could measure the X force with reasonable accuracy when the diameter is horizontal (see Fig. 5). The effect of the other loads

and load position dR is small on the gauges at radius B, and the sensitivity to X is reasonable (> 1 με/kN).

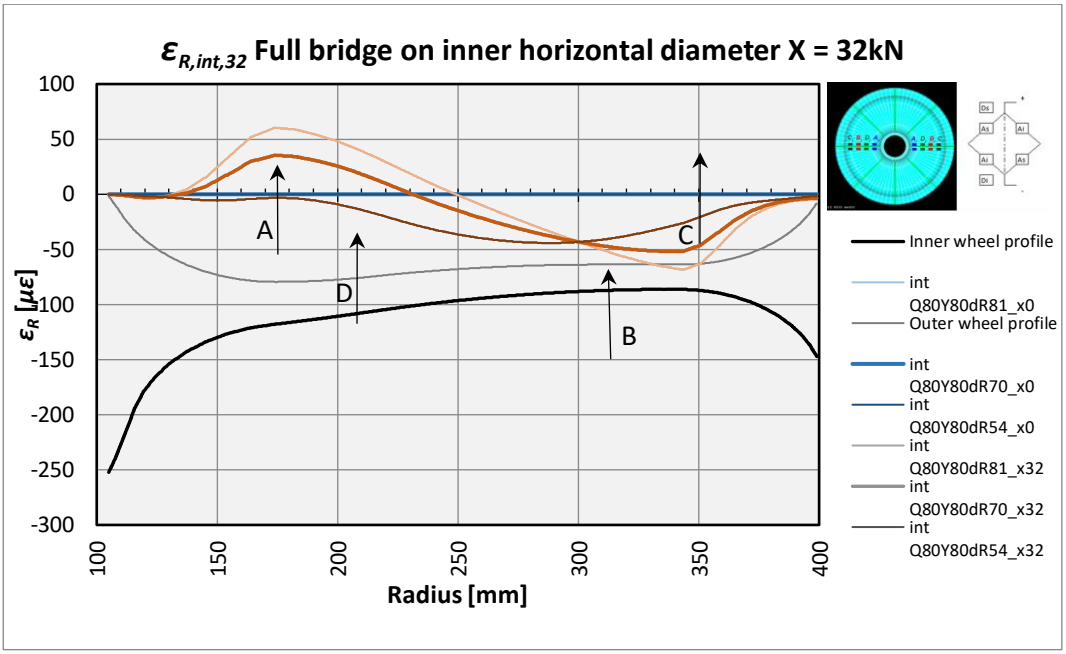

Figure 5 – Equivalent strain for a full bridge on the horizontal (inner side), X = 32kN.

To sum up, the best configuration is judged by the authors to be the 2-channel/wheel full-bridge system, in A and B (referring to Fig. 4), on the inner surface of the wheel with:

- the bridge in A measuring Y when it is in the vertical position (twice per revolution);
- the bridge in B measuring Q when it is vertical and X when it is horizontal, both twice per revolution.

With this configuration, the simulated measurement errors in A, B for each load condition are listed in Tab. 5 and Tab. 6.

Inner side of the wheel, vertical, Full Bridge in B					
Radius [mm]			306.8	306.9	306.8
Simulated strain [με] Load condition Q=70 Y=0 X=0 [kN]			**-261.19**	**-287.51**	**-243.26**
Q [mm]	**Y [mm]**	**dR [mm]**	**"Measured" Y**	**Difference %**	**Square Difference %**
70	00	70	69.26	-0.74	0.55
70	50	70	69.22	-0.74	0.60
70	00	54	76.24	6.24	38.91
70	50	54	76.20	6.20	38.49
70	00	81	64.50	-5.50	30.20
70	50	81	64.47	-5.53	30.56
			Sample std dev %		**5.28**

Table 5 – Measurement errors in Q for Q = 70kN, vertical

Even if the standard deviation on Q is quite relevant, 5.28% as in Tab. 5, and not improvable because of the influence of the contact point [14], [17], [15], the measurement accuracy of Y can be easily improved by compensation of effects of *Q* (Tab. 6). This possibility was explored, by

estimation of the equivalent strain given by *Q* in A, and its subtraction from the strain measured in A.

$$\varepsilon_{A'} = \varepsilon_A - K_{est} \cdot \varepsilon_B$$

The estimated strain in A given by *Q* is calculated through the strain measured in B (function only of *Q*) with a compensation factor K_{est}, which is the ratio between strains given by Q only, evaluated in A and B, for *dR* = 70mm.

$$K_{est} = \frac{\varepsilon_{A,70}}{\varepsilon_{B,70}}$$

Please note that K_{est} would be evaluated when characterising and calibrating the instrumented wheelsets.

Inner side of the wheel, vertical, Full Bridge in A before and after compensation								
Radius [mm]			174.0	174.0	174.0	174.0	174.0	174.0
Simulated strain [με] Load condition: Q=70 Y=0 X=0 [kN]]			**Before compensation**			**After compensation**		
			-1676.44	**-1767.40**	**-1619.74**	**-1761.31**	**-1860.85**	**-1698.80**
Q [kN]	**Y [kN]**	**dR [mm]**	**Measured Y [kN]**	**Diff. [%]**	**Square Diff. [%]**	**Measured Y [kN]**	**Diff. [%]**	**Square Diff. [%]**
70	00	70	-2.41	-2.41	5.80	0.00	0.00	0.00
70	50	70	47.55	-2.45	5.98	49.96	-0.04	0.00
70	00	54	0.03	0.03	0.00	2.68	2.68	7.19
70	50	54	50.13	0.13	0.02	52.79	2.79	7.76
70	00	81	-3.99	-3.99	15.90	-1.74	-1.74	3.04
70	50	81	45.95	-4.05	16.44	48.19	-1.81	3.28
			Sample std dev [%]		**2.97**	**Sample std dev [%]**		**2.06**

Table 6 – Measurement errors in A for Q = 70kN, vertical before and after correction

2.3.2 Dynamic considerations – Peak Detection

The above considerations do not consider the rotation of the wheel under varying loads, and assume that the instrumented diameter is in the best position for measurement (the vertical position for Y and Q, horizontal for X). Some considerations are needed therefore to assess the suitability of the proposed system in terms of sampling the contact force values and detecting impact loads (e.g. joints, frogs) off the correct position of the measurement system.

The most critical aspect regarding sampling is the signal of the bridge 'B' along one wheel revolution. This bridge is used to estimate force components Q and X. The simulated signal obtained from the bridge in the presence of constant loads is shown in Fig. 6. The signal shows a severe peak for points of the circumference close to the lower vertical inner section, which is not present in the signal of bridge 'A' which is almost sinusoidal in shape. This feature poses the problem of having a sampling frequency high enough to accurately capture the peak value.

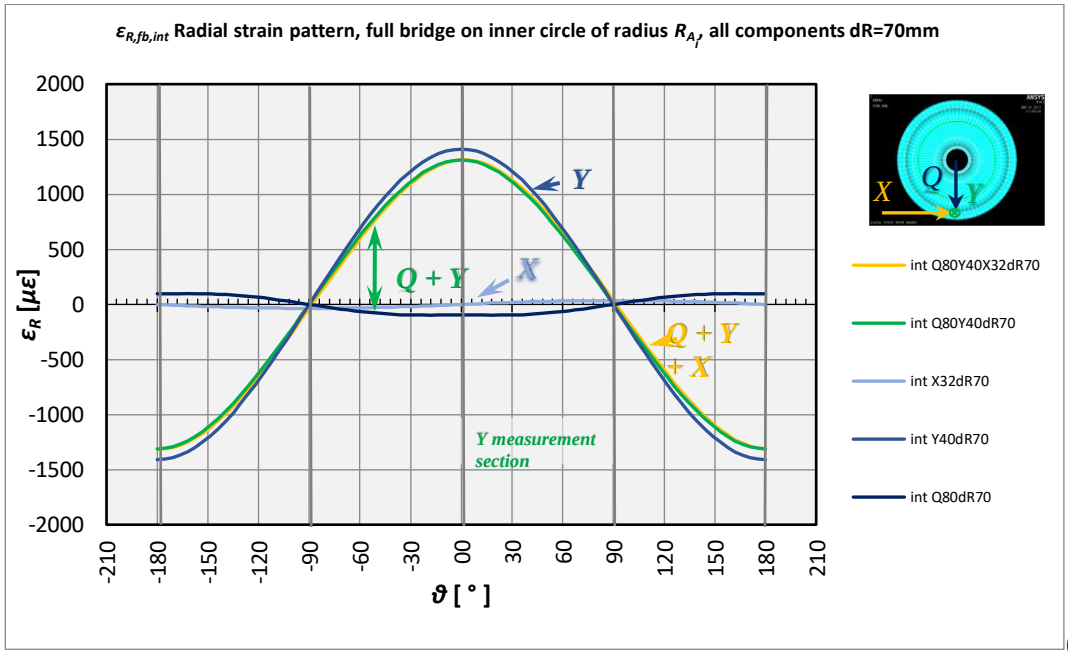

(a)

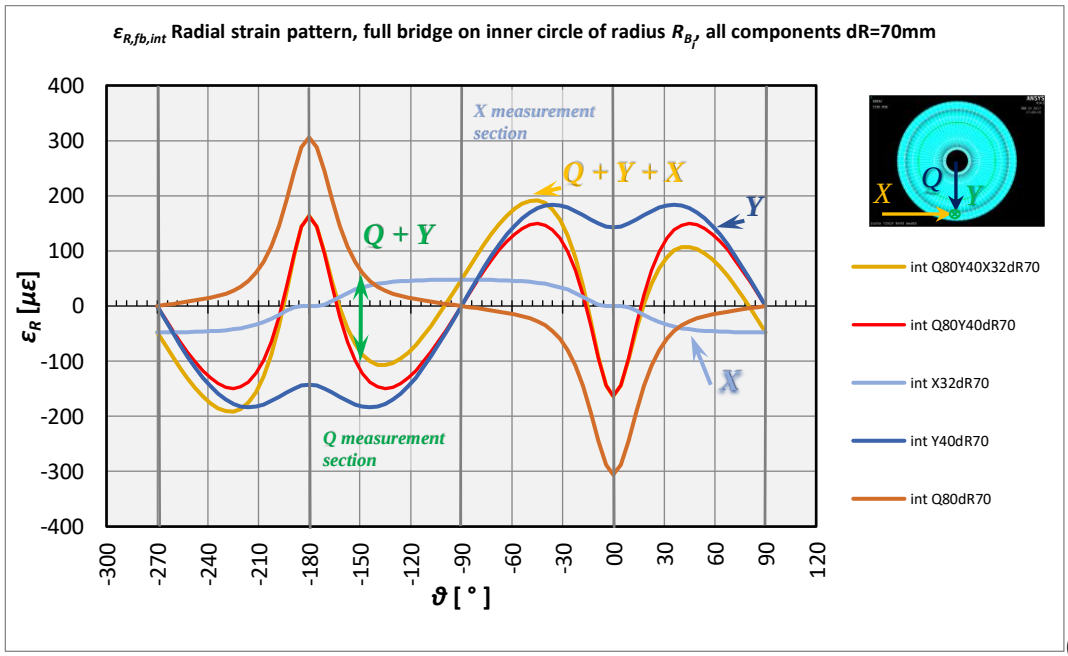

(b)

Figure 6 – (a) radial strains measured along the inner wheelside circumference in A, effect of Q, Y, X; (b) radial strains measured along the inner wheelside circumference in B, effect of Q, Y, X

In previous campaigns, Q (and Y, but this is easier as mentioned) have been successfully sampled up to 160 km/h with peak detection algorithms, at 5 kHz sampling rate [16], [20]. The dynamic component of the signals was shown to be quite low even on poor track geometry and did not affect the sampling [16]. For the WISE-FM application, it is expected that sampling could be performed with a similar technique, and for load spectra reconstruction the possibility of using rainflow counting could be explored. Fig. 6 also shows how the Y and X components really have a negligible effect close to the vertical bridge position, so this potential contribution to the error does not materialise.

Regarding the possibility to detect impact loads, a qualitative answer is given by using the static model in a simple analysis on the wheel revolution (Fig. 7 and Fig. 8). The effect of impact loads on the bridge 'A' signal is assessed statically for different angular positions of the wheel. A square-

wave wheel-load-doubling impact occurring within a crossing (traversed distance of 6 cm) is imagined and the response verified for all load cases. Only the variation of Q due to the crossing is considered, i.e. no alteration of the Y force is assumed. This is a cautious assumption since the presence of Y variations would make the impact loading more detectable. The impact is assumed to be detectable if it generates a signal in equivalent strain of more than a given measurement-chain noise level (10 μm/m is taken, this is a cautious quite pessimistic value).

It is important for at least one of the two bridges A or B to be capable of detecting with a high probability the occurrence of an impact, particularly for the load spectrum application. For this application, at the moment there is no intention to assign a precise force value to the impact, since even the most complex state-of-the-art systems have difficulty in achieving the required bandwidth (>>100 Hz). The current proposal is to assign a cautious conventional value in kN for Y and Q to each counted impact. For the early defect detection application, a wheel defect such as a wheel-flat should be identifiable more easily than a track defect due to its repetitive nature (once per wheel revolution).

The 'A' bridge results for one of the tested load cases for 5 different angular positions of the impact with respect to the wheel are shown (Fig. 7). The bridge is generally sensitive but with 2 «blind spots» (in the proximity of the 90° angular positions) of about 2x15° = 30°/rev. Assuming the impact may occur with the same probability for each point around the wheel circumference, this means that 30/360 = 1/12 impacts could go undetected – in other words more than 90% of impacts would be detected. Experimental tests on a rig would be needed to confirm the extent of this blind spot given the simplifying (but cautious) assumptions used here. Since the nature of the problem leads to a systematic underestimate of the impact count, there is potential to use a statistical correction to compensate for blind-spots.

Bridge 'B' is not very sensitive to impacts (Fig. 8) in several angular positions. Therefore, the use of bridge 'A' is suggested for impact load detection.

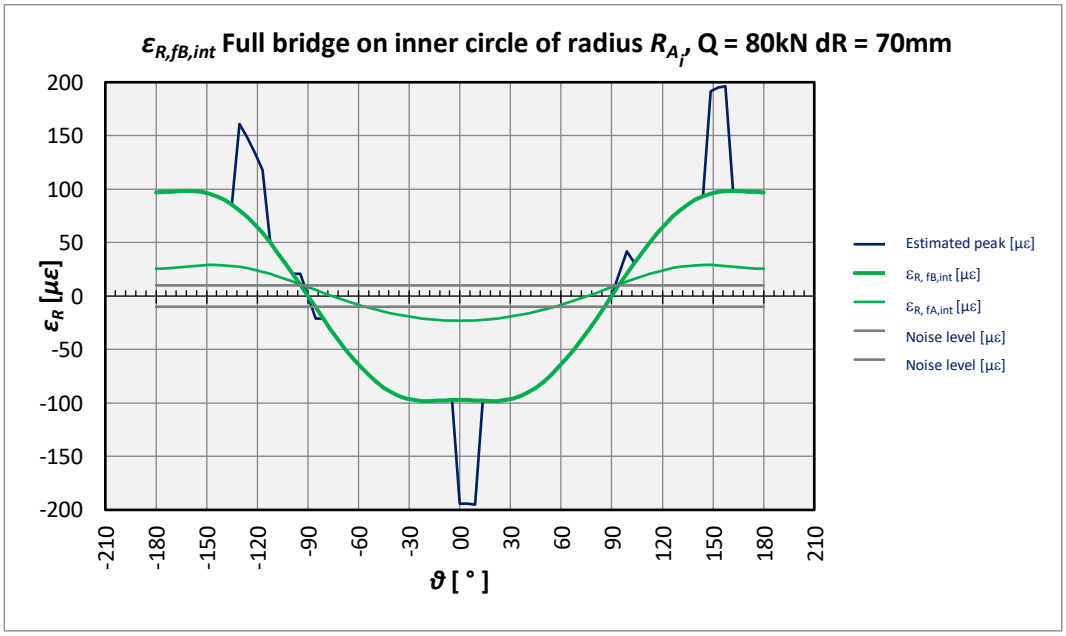

Figure 7 – Full Bridge in A – Q, peak sensitivity; in evidence: (green colour) strains $\varepsilon_{R,fB,int}$ and $\varepsilon_{R,fA,int}$ for inner side of the wheel, (grey colour) strain noise levels, (blue colour) estimated peak for measured strains

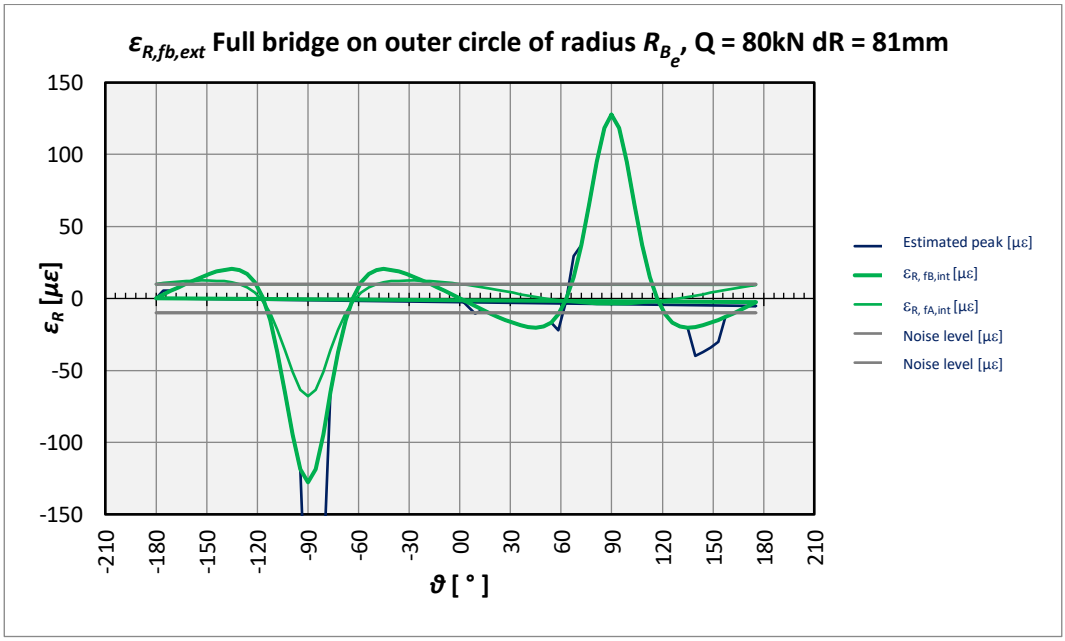

Figure 8 – Full Bridge in B – Q, peak sensitivity: in evidence: (green colour) strains $\varepsilon_{R,fB,int}$ and $\varepsilon_{R,fA,int}$ for outer side of the wheel, (grey colour) strain noise levels, (blue colour) estimated peak for measured strains

It is reckoned that these results are indicative of the actual dynamic behaviour. This issue would of course need further verification, for example with a dynamic FE model (not in the scope of this work) or, better still, by means of full-scale experiments e.g. on a test rig which would eliminate modelling accuracy concerns and include the measurement chain effects, all at a comparable effort. Combining the two assessments (FE and test rig) would also be a more expensive but more robust possibility.

3. SUITABILITY OF THE WISE-FM SYSTEM FOR THE INTENDED APPLICATIONS

In the previous section some indicators related to the accuracy of the proposed force monitoring system are quantified. An error of less than 10% is quantified in all cases, with two full-bridge channels per wheel.

In this subsection we assess how the achievable accuracy meets the minimum requirements in the applications initially identified:

a) increasing design and maintenance effectiveness through a better knowledge of in-service loads;

b) supporting predictive maintenance through the early identification of faults;

c) identifying safety hazards.

In order to perform the assessment for item a), actual load spectra measured in the WIDEM research project were used (wheel of very similar design to that of this case study). The previously calculated errors (Tables 5 and 6) were overlapped to the spectra for Q and Y, taken from Cantini – Beretta [18] and reconstructed in an approximate way, in order to obtain error bands, comparing the magnitude of them to the wheel-rail forces. In addition to that, it was possible to evaluate the uncertainty on the estimation of the number of fatigue cycles derived by the measurement system approximated results.

Particularly for Q (Fig. 9), the error in terms of wheel revolutions at a given load is quite high (one Order of Magnitude) even with a not-so-high error on the load measurement as previously shown. This is due to the shape of the spectrum. The error on the number of wheel revolutions at a given load is lower for Y (Fig. 10) than in the case of Q (< one Order of Magnitude). Considering the use of the load spectra for axle life calculations, since the axle's damage (and consequently its operational life) is more sensitive to Y than Q (see e.g. [17]), the difference in behaviour between Y and Q does not generate substantial errors in life estimation. In fact, this is less than an Order of Magnitude for the most frequent dynamic overloads, as remarked on Fig. 10. For other component-life considerations this issue would have to be further explored.

The measurement error has a significant systematic nature. For example, the higher Y values (refer to Fig. 10) will most likely occur for flange contact. In this condition the proposed WISE-FM system leads to an over-estimate of the Y force due to the effect (see Tab. 6). Therefore, the upper error limit applies. Similar analyses may be performed for the remaining parts of the spectrum and for the Q spectrum.

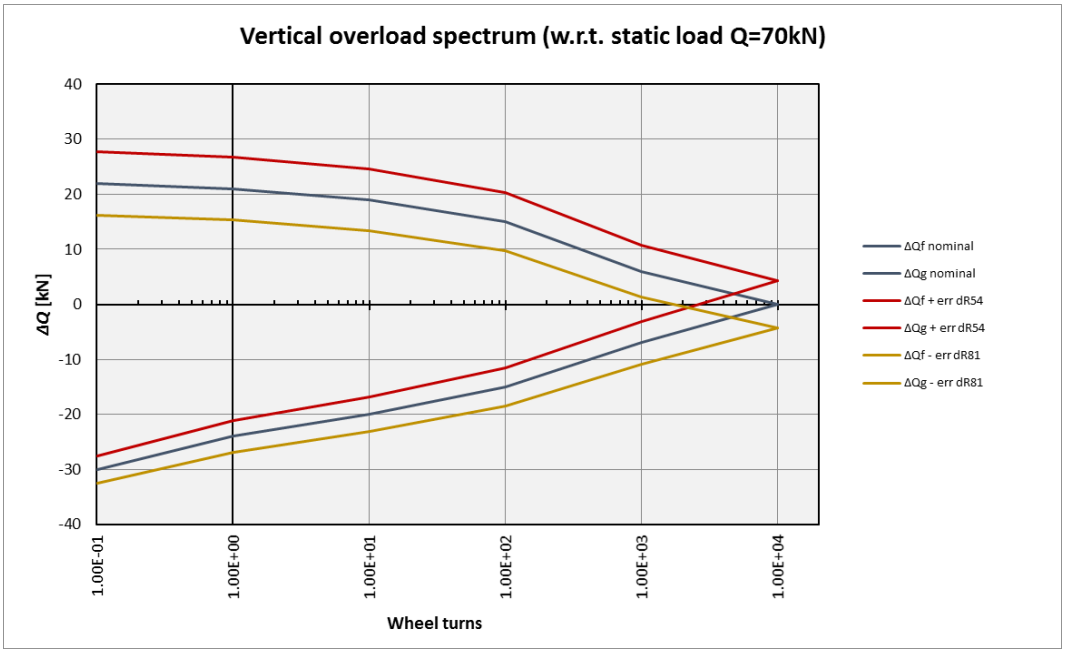

Figure 9 – Error bands corresponding to the proposed WISE-FM system as superposed on a realistic Q overload spectrum coarsely reproduced from Beretta – Cantini [18], to be summed to static load Q = 70kN.

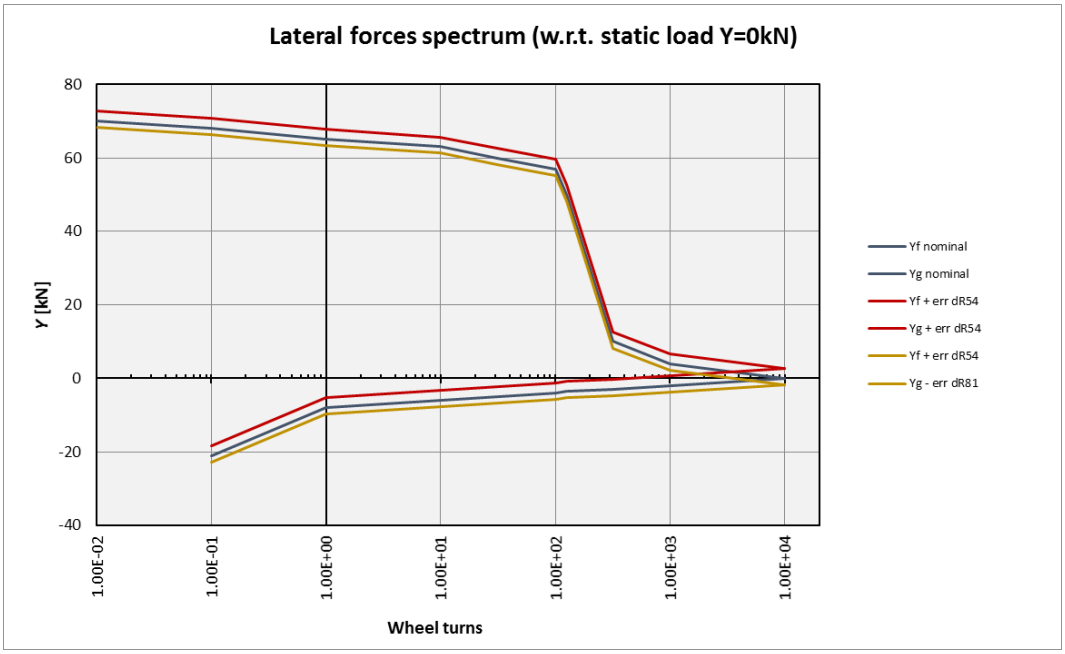

Figure 10 – Error bands corresponding to the proposed WISE-FM system as superposed on a realistic Y load spectrum coarsely reproduced from Beretta – Cantini [18].

In conclusion, due the nature and shape of load spectra, there is a high sensitivity to load measurement error. This would call for extremely high accuracy, probably beyond what is currently possible even with the most sophisticated gauge configurations. In other words, load spectra are a particularly demanding application in terms of required accuracy if the focus is on one single wheel-pair/wheelset. However, this application is not expensive in the sense that only a small fraction of a train fleet may be instrumented under the assumption that the other units of the same type should behave similarly under identical maintenance conditions. The approximate knowledge of the loads matches the approximate load conditions used in component design. If any differences are found, they may be exploited for two strategies with potentially strong economic impacts:

- design changes to components that reach their end of lifetime before the trainset does; an example could be the wheelset, whose mass in a “second series” could be reduced on the basis of actual service loads;
- adaptive maintenance intervals based on the actual service loads; for example, the same vehicle type running on different lines/networks may undergo different inspection intervals such as for ultrasound testing.

Regarding item b) for condition-based maintenance, the main possible uses for a system with 10% accuracy are listed below:

1. Instability caused by wheel tread wear: as wheel wear progresses the shape of the time-history of force Y during a run on straight track would be altered, e.g. a greater number of oscillations/peaks of Y could be detected in a given time; there is a potential either for fixing an upper threshold for Y on straight track or for comparing the time-histories with those of a new wheel (“reference” time history for Y). A 10% accuracy is not ideal for identifying trends due for example to wheel profile wear evolution, but the system should be able to detect larger lateral force variations due to high-speed instability (safety).
2. Damper faults: they can significantly change the running dynamics [10]. A yaw damper fault could cause oscillation increases for both Q, Y, similarly to the related accelerations [18], probably detectable in a short time also with distance-based sampling of forces.

Both the above defects can alter the kinematic wavelengths of lateral/yaw oscillations ("hunting"). Shortened wavelengths are the ones that need to be detected. With 2 samples per revolution (about 2 samples every 3 m of track, with typical wheel diameters), a 6 m kinematic wavelength such as the one obtained with an equivalent conicity of 0.3 for the wheelset used in this study (Klingel's formula) would be detected with 4 samples, probably enough to show the sinusoidal motion.

3. Load unbalance due to suspension defects: should not be difficult to identify provided the variations are measurable with an accuracy of 10%. Wheel load Q is the best force component for this purpose. The presence of unusual lateral forces on straight track would also be easy to detect.

4. Wheel defects: they are of many different types. The most frequently cited are wheel flats and out-of-round. The first one should be quite probably detectable, its peak being detected every wheel revolution particularly on component Q, easily distinguishable from other cases (frogs, joints). The accuracy of the measured force is not important in this case. The latter would be detected if it creates load variations of more than about 10%.

5. Gearbox problems: may also have an effect on contact forces that has to be studied before concluding on the potential for force monitoring to identify them.

To sum up, WISE-FM could be useful for running-gear condition-based maintenance. Some purposes addressed could be the following (see Tab. 7).

- Monitoring of trends. An example is studying the trends of contact forces due to wheel profile wear as a support to reprofiling strategies. It may not be necessary to instrument the whole fleet. A study about the accuracy of the measurement (here evaluated in the order of 10%), could be considered in further developments.

- Early identification of faults, "early" meaning enough in advance to implement corrective actions. The fault modes addressed would depend on the priority given by the vehicle operator (e.g. most frequent ones). Wheel flats, some damper faults and load unbalances should be detectable with the WISE-FM system. This type of application requires instrumentation of all wheels of the train fleet. Potential benefits are the better management of workshop slots and availability improvement of the trainsets, their running gear condition and lower aggressiveness towards the track. Moreover, WISE-FM could be a validation method of new materials, active systems and more effectively designed components, addressed to a risk mitigation method, to maintain an acceptable level of risk in the sense of EU legislation.

Finally, safety applications could also be of two types.

- Monitoring of trends. An example is that of the application of Matsumoto et al. [7], in which the derailment ratio is monitored on one trainset as a risk mitigation measure. This type of application may not require full-time monitoring but only in critical periods, as reported in [21]. The traction ratio on the inner wheel could also be monitored. For both the above applications a 10% accuracy is sufficient.

- Early identification of faults/hazards. Examples of this application are instability detection and derailment detection, on a train fleet. Such applications can generate slow-downs or train-trips in regular service, however. The latter are particularly demanding for the monitoring system, since any fault in the monitoring system, on any wheel/wheelset of the train, would trip the train even in the absence of a hazard. The unavailability requirements are such that some form of redundancy is required, along with algorithms judging rapidly

when one of the redundant channels needs to be shut down because it is faulty. Further studies would have to show whether the number of channels on the wheel would have to be multiplied. With triplex redundancy, 6 channels would be required, with independent transducers, telemetry, wiring. This would complicate the system to a point that is beyond the level of simplicity that was imagined when starting this research.

For all of the above applications, algorithms need to be developed. A possibility is for the algorithm to compare actual values of contact forces to benchmark time histories, e.g. with new, partially worn, completely worn profiles. Otherwise forces could be compared with well-defined thresholds.

Separate mention is given to the longitudinal force X. In addition to creating a load distribution estimation also for this component and improving wheelset design, several potential developments can be recognised, all requiring further study:

a. failure detection improvement, the actual X and its variation could be used as additional criterion for failure detection or confirmation through reconstruction of the contact force vector;

b. it could contribute to the detection of yaw damper problems in combination with Y;

c. quasi real-time adhesion coefficient estimation should be possible with a 10% accuracy, thus improving tractive effort management, and replacing or integrating the systems are currently used with the same purpose, generally wheel/rotor speed control.

This opens the door to another application, which is the provision of feedback control signals for future active steering systems (Tab. 7).

4. CONCLUSIONS

The research described in this paper has shown that it is feasible, at least for the wheel type used as a case study, to obtain measurements of wheel loads X, Y and Q with an accuracy of the order of 10% with a system that has a good potential for widespread and durable application on trains in service. The WISE-FM system requires 2 strain-gauge channels per wheel and may use durable hardware that is not yet Commercial Off-The-Shelf but has seen long-distance practical implementation in-service. It may even be possible to limit the system to 3 channels per wheelset through equilibrium considerations (to be explored eventually in subsequent research). It may be used with both solid-axle wheelsets and Independently Rotating Wheels. For many potential applications only a few trainsets of a fleet could be instrumented with benefits for the whole fleet, for other ones the whole fleet should be equipped. Considerations about it would be developed in a separate study, including e.g. channel redundancy, diagnostics and so on.

The initial intended application of the system was to generate in-service load distributions to inform re-design for the reduction of unsuspended masses and enable maintenance plans that adapt to the actual service conditions. The analysis described in this paper shows that this is possible both for the quasi-static and dynamic force components (e.g. impacts on frogs, joints etc. which are an important part of a load distribution). The forces cannot be measured accurately on these elements, but they can be counted and assigned a conventional (high) load value. Due the nature and shape of load distributions, there is a high sensitivity to load measurement error. This would call for extremely high accuracy, probably beyond what is currently possible even with the most sophisticated gauge configurations.

Purpose Level 1	Level 2	Level 3	Wheels instrumented	Remarks on the feasibility with 10% accuracy
in-service loads	improved design	lower unsprung mass in subsequent design	only leading wheelset on a few trainsets	although the accuracy on the number of cycles is not high, the force information collected would still be valuable for the purpose
	adaptive maintenance	maintenance/inspection intervals adapted to service/line	only leading wheelset on a few trainsets	although the accuracy on the number of cycles is not high, the force information collected would still be valuable for the purpose
condition-based maintenance	monitoring trends	support for maintenance/inspection intervals	only selected wheels	probably difficult to detect slow variations due to vehicle condition
	early detection of faults for better workshop management, reduced operational unavailability, improved average running condition	wheel flats	all	a high accuracy is not necessary; even though the system is distance-based it should be able to identify force peaks that occur at precise angular positions due to flats
		yaw damper faults	all	the combined effect on lateral and vertical forces should be able to allow detection
		other damper faults	all	not all dampers would necessarily lead to detectable force variations
		faults creating load unbalances (springs, other elements)	all	should be quite easily detected
		out-of-round	all	distance based sampling may not be adequate for some forms
		wheel wear	all	might not lead to detectable force variations, depending on the severity of the problem
running safety	monitoring trends	alerts in periods when conditions are unfavourable (e.g. derailment ratio, traction ratio)	only leading wheelset on one or few trainsets	the system should be quite suitable for this type of application
	early detection of hazards	train-trip/slow for faults creating unusally high contact forces, enabler of novel running-gear technology	all wheels	high contact forces and variations are certainly easy to detect with the system, although the high redundancy probably required would complicate the setup
feedback signals	traction control	force feedback signals for difference with desired force	all motorised wheels	the system should be quite suitable for this type of application
	active steering	force feedback signals for difference with desired force	all actively-steered wheels	the system is probably suited, but high redundancy level is probably required

Table 7 – Feasibility according to the purpose of WISE-FM.

However, the knowledge, albeit approximate, of in-service loads on a variety of different trains would allow e.g. the understanding of:

- the variability between trainset and trainset of a given type running on the same lines;
- the variability between trainsets of a given type running on different lines.

Considerations on how the knowledge of approximate wheel load distributions could support the design of other parts than the wheelset (bogie frames, axle-boxes, gearboxes etc.) could be usefully further explored. This could be particularly important for the introduction of novel materials.

The reduction of unsuspended mass could be exploited for example at the end of the lifetime of the first wheelsets, which could be replaced by lighter redesigned ones, with benefits for vehicle and track maintenance, energy consumption and passenger revenue. This might apply to other components. The possibility is particularly attractive in these times of hopefully rapid innovation thanks to the SHIFT2RAIL programme, as it could enable quicker time-to-market and troubleshooting of novel designs, plus the easier introduction of design changes during the lifetime of a product.

Adaptive maintenance plans could be initiated already after the first months of monitoring. Inspection and replacement intervals could be adjusted on the basis of the measured loads.

The other potential uses are for condition-based maintenance and hazard identification, and for provision of control signals.

With a 10% accuracy, WISE-FM potentially allows the identification of several types of defects on the wheelset itself but also on suspension and drive-train elements. Any fault that would cause a load variation of more than 10% for about half a wheel revolution should be detectable in principle: variations in stiffness of suspension elements and other suspension defects, some forms of out-of-round, instability, damper faults e.g. yaw dampers, possibly gearbox faults. This type of application would require all wheelsets to be instrumented, and could benefit from the parallel use of different systems to make identification more robust (e.g. accelerometers on the bogie frame or the gearboxes to identify their defects).

Another possibility is a frequent traction ratio and adhesion coefficient estimation allowing a better understand of its daily and seasonal variations.

Regarding safety-related applications, the derailment ratio and adhesion coefficient measurement is one possibly useful contribution which would only require a few wheelsets to be instrumented. If all, or all critical, wheelsets are instrumented, a 10% accuracy force measurement would of course be capable of detecting running safety hazards which would almost certainly generate large force variations (e.g. derailment detection for high-speed applications). This type of application is quite challenging since it has important effects not only on safety but also on operational availability (false alarms would generate train trips or slow-downs). Therefore, harsh reliability-availability requirements would need to be applied with redundancy in the sensors and the measurement chain that could make the system much more complex.

This study identifies WISE-FM as potential enabler of three technological breakthroughs that could bring great benefits to railways and thus contribute to a favourable modal shift towards this safe and green mode:

- adaptive maintenance based on actual service loads;
- the introduction of new materials particularly in the unsuspended running-gear parts;
- active steering systems.

Further research is needed for the following aspects:

- to assess the impacts (e.g. costs and benefits for a specific operator or type of operator) in order to decide which applications are most promising;
- to prove the system experimentally;
- to generate the algorithms depending on the selected applications.

All in all, the WISE-FM single system could offer a wide variety of functions classifiable as in-service load monitoring, early defect detection, hazard identification and provision of feedback signals.

5. ACKNOWLEDGEMENTS

The RUN2Rail project has received funding from the Shift2Rail Joint Undertaking under the European Union's Horizon 2020 research and innovation programme under grant agreement No 777564.

REFERENCES

[1] D. E. OTTER, M. A. EL-SIBAIE e R. L. HIGGINS, «A design for next generation load measuring wheel sets.,» in *Proceedings of the 1991 IEEE/ASME Joint Railroad Conference.*, 1991.

[2] CEN, *NF EN 14363 - Railway applications - Testing for the acceptance of running characteristics of railway vehicles.,* CEN, December 2005.

[3] M. ALESSANDRIA, B. DOTTA e R. LICCIARDELLO, «Long-term contact force measurements with the CML method,» *Ingegneria Ferroviaria,* vol. 66, pp. 929-948, 2011.

[4] CEN, *TSI LOC&PAS - Regolamento (UE) n. 1302/2014,* European Railway Agency, 2014.

[5] S. CANTINI e S. BERETTA, Structural reliability assessment of railway axles., 2011: Lucchini RS.

[6] S. BRUNI, R. GOODALL, T. X. MEI e H. TSUNASHIMA, «Control and monitoring for railway vehicle dynamics.,» *Vehicle System Dynamics,* vol. 45, n. 7-8, pp. 743-779, 2007.

[7] A. BRACCIALI, F. CAVALIERE e M. MACHERELLI, «Review of instrumented wheelset technology and applications.,» in *Proc. 2nd Int. Conf. Railway Technol., Res., Develop., Maintenance.*, 2014.

[8] G. R. CORAZZA , G. Malavasi, R. Licciardello e M. Marcone, «La ruota come sensore d'interazione ruota-rotaia.,» *Ingegneria Ferroviaria,* n. 3, pp. 119-131, 1999.

[9] A. MATSUMOTO, Y. Sato, H. Ohno, M. Tomeoka, K. Matsumoto, J. Kurihara e & Nakai, T., «A new measuring method of wheel–rail contact forces and related considerations.,» *Wear,* vol. 265, n. 9-10, pp. 1518-1525, 2008.

[10] T. X. MEI e X. J. DING, «A model-less technique for the fault detection of rail vehicle suspensions.,» *Vehicle System Dynamics,* vol. 46, n. S1, pp. 277-287, 2008.

[11] M. BRUNER, G. CORAZZA, E. COSCIOTTI, R. LICCIARDELLO e G. MALAVASI, «Y- und Q- Kräftmessung: Analyse und Feldfahrungen eines neuen Verfahrens,» *ZEV rail Glasers Annalen,* vol. 128, pp. 272-277, 2004.

[12] SHIFT2RAIL, «Multi-Annual Action Plan,» 2015.

[13] UNI, *UNI EN 13103-1:2018 Applicazioni ferroviarie - Sale montate e carrelli - Parte 1: Metodo di progettazione per assi con boccole esterne,* UNI, 2018.

[14] UNI, *UNI EN 13260:2011 Applicazioni ferroviarie - Sale montate e carrelli - Sale montate - Requisiti del prodotto,* UNI, 2011.

[15] M. ENTEZAMI e et. al., «Perspectives on railway axle bearing condition monitoring.,» *Proceedings of the Institution of Mechanical Engineers, Part F: Journal of Rail and Rapid Transit,* p. 0954409719831822, 2019.

[16] D.-H. e. a. LEE, «Development of condition monitoring system for reduction unit of high-speed rail.,» *Journal of the Korean Society for Precision Engineering,* vol. 30, n. 7, pp. 667-672, 2013.

[17] S. e. a. BRUNI, «Road test data procedures for evaluating the hunting instability threshold of a railway vehicle from on board measurements.,» *Vehicle System Dynamics,* vol. 33.sup1, pp. 168-179, 1999.

[18] L. GASPARETTO, S. ALFI e S. BRUNI, «Data-driven condition-based monitoring of high-speed railway bogies.,» *International Journal of Rail Transportation-,* vol. 1, n. 1-2, pp. 42-56, 2013.

[19] M. BRUNER, G. B. BROGGIATO e R. V. LICCIARDELLO, «Studio numerico - sperimentale delle deformazioni di una sala ferroviaria di misura,» in *XXXII Congresso AIAS (Associazione Italiana per l'Analisi delle Sollecitazioni)*, 2003.

[20] F. Savin e F. Braghin, «Project no. TST-CT-2005-516196 - Wheelset integrated design and effective maintenance - D2.1 Load spectra for two service profiles to be used in new design,» WIDEM, 2008.

[21] A. MATSUMOTO, S. YASUHIRO e O. HIROYUKI, «A new monitoring method of train derailment coefficient,» *QR,* pp. 136 - 140, 2002.